

# Blueshifted light from the last-scattering epoch

Andrzej Krasiński,

N. Copernicus Astronomical Center, Warsaw, Poland

## Contents

1	Motivation and background	2
2	The Lemaître – Tolman (L–T) models	3
3	Light rays in LT models	5
4	The redshift	6
5	The extremum-redshift hypersurface	8
6	The quasi-spherical Szekeres (QSS) models	10
7	Blueshifts in QSS metrics	13
8	Adapting the BB profile to generating strong blueshift	14
9	Explaining the brief durations of the GRBs	18
10	Expression of hope	19
11	Appendix: Blueshifts in exemplary QSS models	20

## 1. Motivation and background

The Lemaitre [1] – Tolman [2] (L-T) and Szekeres [3] (Sz) models are the simplest exact generalizations of the Friedmann-class metrics.

The Big Bang (BB) in them is in general non-simultaneous in comoving coordinates.

Some light rays emitted at the BB in these models display **infinite blueshift** rather than infinite redshift (see further).

This happens when the BB function  $t_b(r)$  has  $dt_b/dr \neq 0$  at the emission point and the ray propagates radially (in L-T) or along one of two preferred directions (in Sz).

→ Rays emitted during the **last scattering period** ( $\approx 380\,000$  years after the BB) may have **finite blueshift**.

Can such rays be now observed?

**Yes!** – in principle. I will argue that they might be among the gamma-ray bursts.

[1] G. Lemaître, L'Univers en expansion [The expanding Universe], *Ann. Soc. Sci. Bruxelles* **A53**, 51 (1933); *Gen. Rel. Grav.* **29**, 641 (1997).

[2] R. C. Tolman, Effect of inhomogeneity on cosmological models, *Proc. Nat. Acad. Sci. USA* **20**, 169 (1934); *Gen. Rel. Grav.* **29**, 935 (1997).

[3] P. Szekeres, A class of inhomogeneous cosmological models. *Commun. Math. Phys.* **41**, 55 (1975).

## 2. The Lemaître – Tolman (L-T) models

This class of solutions of Einstein's equations follows when we assume that

*1. The spacetime is spherically symmetric.*

*2. The source in the Einstein equations is dust* (pressure = 0).

→ The metric and velocity field of the dust , in comoving coordinates, have the form:

$$ds^2 = dt^2 - e^{A(t,r)} dr^2 - R^2(t, r)(d\vartheta^2 + \sin^2 \vartheta d\varphi^2), \quad (2.1)$$

$$u^\alpha = \delta^\alpha_0. \quad (2.2)$$

$A(t, r)$  and  $R(t,r)$  are to be found from Einstein's equations.

$$ds^2 = dt^2 - e^{A(t,r)} dr^2 - R^2(t,r)(d\vartheta^2 + \sin^2 \vartheta d\varphi^2),$$

$$u^\alpha = \delta^\alpha_0.$$

The solution of Einstein's equations with  $R_{,r} \neq 0$  is

$$ds^2 = dt^2 - \frac{R_{,r}^2}{1 + 2E(r)} dr^2 - R^2(t,r) (d\vartheta^2 + \sin^2 \vartheta d\varphi^2) \quad (2.3)$$

where  $E(r)$  is arbitrary and  $R(t,r)$  is determined by

$$R_{,t}^2 = 2E(r) + \frac{2M(r)}{R} - \frac{1}{3}\Lambda R^2, \quad \rightarrow \text{solution depends on } t - t_B(r). \quad (2.4)$$

$M(r)$  and  $t_B(r)$  are arbitrary, and the mass density is

$$\frac{8\pi G}{c^2} \rho = \frac{2M_{,r}}{R^2 R_{,r}}. \quad (2.5)$$

This solution was found by Lemaître [1] in 1933, then interpreted by Tolman [2] in 1934 and Bondi [4] in 1947

(and investigated by > 100 other authors later. The number is still growing.)

[1] G. Lemaître, L'Univers en expansion [The expanding Universe], *Ann. Soc. Sci. Bruxelles* **A53**, 51 (1933); *Gen. Rel. Grav.* **29**, 641 (1997).

[2] R. C. Tolman, Effect of inhomogeneity on cosmological models, *Proc. Nat. Acad. Sci. USA* **20**, 169 (1934); *Gen. Rel. Grav.* **29**, 935 (1997).

[4] H. Bondi, Spherically symmetrical models in general relativity. *Mon. Not. Roy. Astr. Soc.* **107**, 410 (1947; *Gen. Rel. Grav.* **31**, 1783 (1999).

$$ds^2 = dt^2 - \frac{R_{,r}^2}{1 + 2E(r)} dr^2 - R^2(t, r) (d\vartheta^2 + \sin^2 \vartheta d\varphi^2) \quad (2.3)$$

### 3. Light rays in L–T models

The partly integrated null geodesic equations in this model are:

$$\frac{dt}{d\lambda} = k^t, \quad (3.1)$$

$$\frac{dk^t}{d\lambda} = \left[ \frac{C^2}{R^2} - (k^t)^2 \right] \frac{R_{,tr}}{R_{,r}} - \frac{C^2 R_{,t}}{R^3}, \quad (3.2)$$

$$\frac{dr}{d\lambda} = k^r, \quad (3.3)$$

$$(k^t)^2 = \frac{R_{,r}^2 (k^r)^2}{1 + 2E} + \frac{C^2}{R^2} \quad (3.4)$$

$$R^2 \sin^2 \vartheta k^\varphi = J_0, \quad (3.5)$$

$$R^4 (k^\vartheta)^2 \sin^2 \vartheta + J_0^2 = C^2 \sin^2 \vartheta, \quad (3.6)$$

$J_0$  and  $C$  are constants. When  $C = 0$ , the geodesic is radial.

The following can be achieved at any  $t_0$  by rescaling  $\lambda$ :

$$k^t(t_0) = \pm 1, \quad (3.7)$$

(+ for future-directed, - for past-directed rays).

$$k^t(t_o) = \pm 1, \quad (3.7) \quad (k^t)^2 = \frac{R_{,r}^2 (k^r)^2}{1 + 2E} + \frac{C^2}{R^2} \quad (3.4)$$

## 4. The redshift

Let event  $e$  be the emission of an electromagnetic wave, event  $o$  – its observation.

The quantity  $z$  defined by:

$$1 + z \stackrel{\text{def}}{=} \frac{\lambda_o}{\lambda_e} \equiv \frac{\nu_e}{\nu_o} = \frac{(k_\alpha u^\alpha)_e}{(k_\alpha u^\alpha)_o} \quad (4.1)$$

is called **redshift** ( $u^\alpha$  is 4-velocity of the emitter/observer).

In comoving coordinates ( $u^\alpha = \delta^\alpha_0$ ) using (3.7), we have

$$1 + z = \pm k^t_e \quad (4.2)$$

(+ for future-directed, - for past-directed rays).

In cosmology, usually  $\lambda_o > \lambda_e$  (so  $z > 0$ ), hence **red**shift, but see further.

On nonradial rays ( $C \neq 0$ ), from (3.4) and (4.2)

$$\lim_{R \rightarrow 0} |k^t| \equiv \lim_{R \rightarrow 0} z = \infty. \quad (4.3)$$

→ **On nonradial rays from the BB  $z \rightarrow \infty$  for all observers,**

→  **$z < 0$  at the present observer is possible only on radial rays.**

$$1 + z = \frac{\nu_e}{\nu_o} \quad (4.1)$$

Let a **radial** ray go to the past from  $P_o$  and hit the BB at  $P_e$ .

Perturbative [5] and numerical [6] calculations both show that on such rays

$$z \xrightarrow{R \rightarrow 0} -1 \quad \text{when } dt_B/dr \neq 0 \text{ at } P_e$$

$$z \xrightarrow{R \rightarrow 0} \infty \quad \text{when } dt_B/dr = 0 \text{ at } P_e$$

$$z \rightarrow -1 \rightarrow \nu_o \rightarrow \infty \text{ when } \nu_e < \infty.$$

The property  $z < 0$  is called **blueshift** [7]; when  $z = -1$  the blueshift is called infinite.

→ On radial rays emitted just after the BB  $\nu_o$  can be larger than  $\nu_e$ .

[5] C. Hellaby and K. Lake, The redshift structure of the Big Bang in inhomogeneous cosmological models. I. Spherical dust solutions. *Astrophys. J.* **282**, 1 (1984) + erratum *Astrophys. J.* **294**, 702 (1985).

[6] A. Krasinski, Blueshifts in the Lemaître – Tolman models. *Phys. Rev.* **D90**, 103525 (2014).

[7] P. Szekeres, Naked singularities. In: *Gravitational Radiation, Collapsed Objects and Exact Solutions*. Edited by C. Edwards. Springer (Lecture Notes in Physics, vol. 124), New York, pp. 477 -- 487 (1980).

$$\frac{dk^t}{d\lambda} = \left[ \frac{C^2}{R^2} - (k^t)^2 \right] \frac{R_{,tr}}{R_{,r}} - \frac{C^2 R_{,t}}{R^3} \quad (3.2)$$

$$k^r = \pm \frac{\sqrt{1+2E}}{R_{,r}} \sqrt{(k^t)^2 - \frac{C^2}{R^2}} \quad (3.4a)$$

$$1+z = \pm k_e^t \quad (4.2)$$

## 5. The extremum-redshift hypersurface

Along a radial ray,  $dr/d\lambda \equiv k^r \neq 0$  and  $C = 0$ .

Then, using (4.2), Eqs. (3.2) and (3.4a) imply

$$\frac{1}{1+z} \frac{dz}{dr} = \pm \frac{R_{,tr}}{\sqrt{1+2E}} \quad (5.1)$$

→  $R_{,tr} = 0$  is the locus of local extrema of  $z$  along rays.

This locus is the **extremum-redshift hypersurface** (ERH).

It is observer-independent and can be calculated numerically.

In the Friedmann limit, the ERH does not exist, but formally may be thought of as coinciding with the BB.



Consider a ray proceeding *to the past* from a point that lies later than the ERH.

$z$  on it increases from 0 at observer to a local maximum at the ERH.

Further to the past,  $z$  *initially* decreases.

The ERH may have a nontrivial geometry  $\rightarrow$  a ray may intersect it several times and have several local maxima and minima. Examples will follow.

At the BB,  $z$  would either decrease to -1 or increase to  $\infty$ .

But L–T models do not apply at times before the last-scattering hypersurface (LSH) because of  $p = 0$ .

*Can  $z$  from the LSH be sufficiently negative to shift the optical frequencies to the gamma-range?*

Yes – when the function  $t_B(r)$  is suitably chosen.

Note: the blueshift is acquired only below the ERH.

Wherever the ray flies above the ERH, it gets only redshifted.

## 6. The quasi-spherical Szekeres (QSS) models

Szekeres [3,8] in 1975 took the following Ansatz for the metric

$$ds^2 = dt^2 - e^{2\alpha} dz^2 - e^{2\beta} (dx^2 + dy^2) , \quad (6.1)$$

$\alpha(t,x,y,z)$  and  $\beta(t,x,y,z)$  to be determined from Einstein's equations with dust source.

Then he found all such solutions.

One sub-family of his metrics generalizes L–T, these are called *quasi-spherical*.

General Szekeres models have *no symmetry*.

[3] P. Szekeres, A class of inhomogeneous cosmological models. *Commun. Math. Phys.* **41**, 55 (1975).

[8] P. Szekeres, Quasispherical gravitational collapse. *Phys. Rev.* **D12**, 2941 (1975).

The QSS solutions have the metric [9]

$$ds^2 = dt^2 - \frac{\mathcal{E}^2(\Phi/\mathcal{E})_{,r}^2}{1 + 2E(r)} dr^2 - \frac{\Phi^2}{\mathcal{E}^2} (dx^2 + dy^2), \quad (6.2)$$

$$\mathcal{E} \stackrel{\text{def}}{=} \frac{(x - P)^2}{2S} + \frac{(y - Q)^2}{2S} + \frac{S}{2},$$

where  $E(r)$ ,  $M(r)$ ,  $P(r)$ ,  $Q(r)$  and  $S(r)$  are arbitrary functions, and  $\Phi(t, r)$  obeys

$$\Phi_{,t}^2 = 2E(r) + \frac{2M(r)}{\Phi} + \frac{1}{3}\Lambda\Phi^2. \quad (6.3)$$

The mass density is

$$\kappa\rho = \frac{2(M/\mathcal{E}^3)_{,r}}{(\Phi/\mathcal{E})^2(\Phi/\mathcal{E})_{,r}}, \quad \kappa = \frac{8\pi G}{c^2}. \quad (6.4)$$

The solution of (6.3) is

$$\int_0^\Phi \frac{d\tilde{\Phi}}{\sqrt{2E + 2M/\tilde{\Phi} + \frac{1}{3}\Lambda\tilde{\Phi}^2}} = t - t_B(r). \quad (6.5)$$

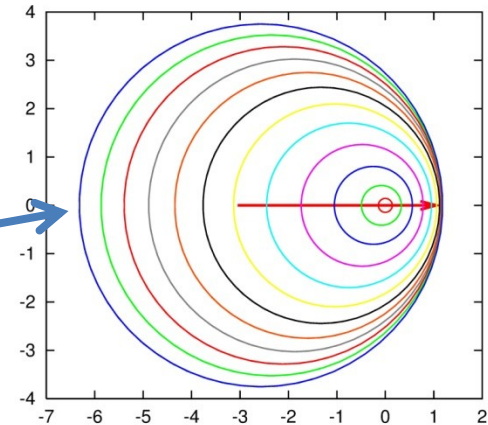
$$ds^2 = dt^2 - \frac{\mathcal{E}^2(\Phi/\mathcal{E})_{,r}^2}{1 + 2E(r)} dr^2 - \frac{\Phi^2}{\mathcal{E}^2} (dx^2 + dy^2), \quad \mathcal{E} = \frac{(x - P)^2}{2S} + \frac{(y - Q)^2}{2S} + \frac{S}{2} \quad (6.2)$$

$$\Phi_{,t}^2 = 2E(r) + \frac{2M(r)}{\Phi} + \frac{1}{3}\Lambda\Phi^2. \quad (6.3) \quad \int_0^\Phi \frac{d\tilde{\Phi}}{\sqrt{2E + 2M/\tilde{\Phi} + \frac{1}{3}\Lambda\tilde{\Phi}^2}} = t - t_B(r). \quad (6.5)$$

The surfaces of constant  $t$  and  $r$

$$ds^2 = \frac{\Phi^2}{\mathcal{E}^2} (dx^2 + dy^2)$$

are **nonconcentric spheres**,  
 $x$  and  $y$  are stereographic coordinates on them.



The L-T models are the limit of constant  $(P, Q, S)$  – then the spheres become concentric and the spacetime becomes spherically symmetric.

## 7. Blueshifts in QSS metrics

In QSS metrics, strong blueshifts exist only along two opposite directions.

(This was determined numerically in exemplary models [10]. General proof still missing.)

In axially symmetric QSS, these directions coincide with the symmetry axis [10].

Can blueshifted rays of QSS models be observed as *gamma-ray bursts* (GRBs)?

Models of GRB sources must account for [11]:

- (1) The observed frequency range of the GRBs ( $0.24 \times 10^{19} \text{Hz} \leq \nu \leq 1.25 \times 10^{23} \text{Hz}$ );
- (2) Their limited duration (up to 30 hours, mostly around 2 minutes [12]);
- (3) The existence and duration of afterglows (typically a few days, max.  $n \times 100$  [13]);
- (4) (Hypothetical) collimation of the GRBs into narrow jets.
- (5) The large distances to their sources ( $n \times 10^9$  ly);
- (6) The multitude of the observed GRBs (nearly 1 per day).

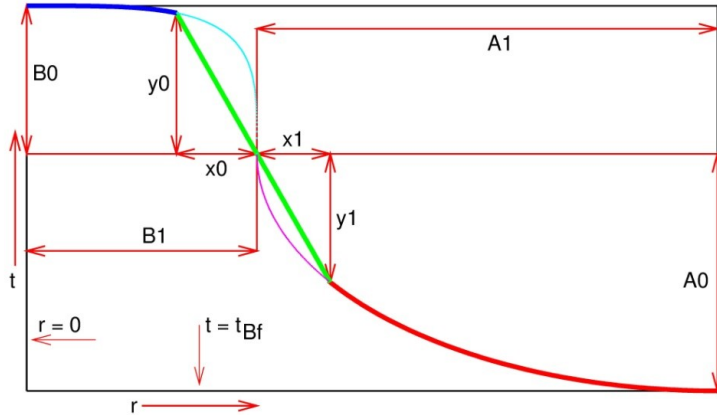
[10] A. Kasiński, Existence of blueshifts in quasi-spherical Szekeres spacetimes. *Phys. Rev.* **D94**, 023515 (2016).

[11] Gamma-Ray Bursts, [http://swift.sonoma.edu/about\\_swift/grbs.html](http://swift.sonoma.edu/about_swift/grbs.html)

[12] <https://imagine.gsfc.nasa.gov/science/objects/bursts1.html>

[13] <http://astronomy.swin.edu.au/cosmos/G/gamma+ray+burst+afterglow>

## 8. Adapting the BB profile to generating a sufficiently strong blueshift



A source of a blueshifted ray is a hump on a constant- $t_B(r)$  background (a finite-size QSS region embedded in Friedmann).

← The hump profile consists of two arcs connected by a straight segment.

Friedmann BB background →

The upper arc is a segment of the curve:

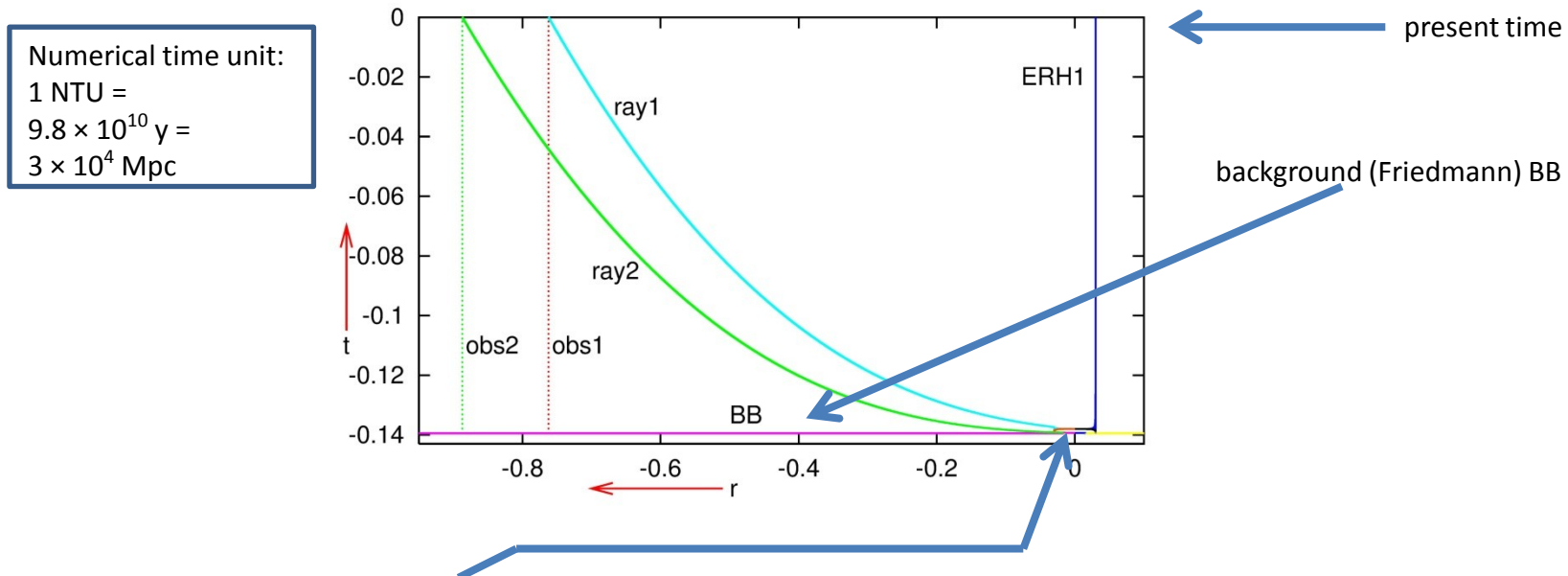
$$\frac{r^n}{B_1^n} + \frac{(t - t_{Bf} - A_0)^n}{B_0^n} = 1 \quad \text{where } n = 4 \text{ or } 6. \quad (8.1)$$

The lower arc is a segment of an ellipse ( $n = 2$ ).

The straight segment prevents  $dt_B/dr \rightarrow \infty$  at the junction of full arcs.

The free parameters are  $A_0$ ,  $A_1$ ,  $B_0$ ,  $B_1$  and  $x_0$ .

**Note: all this material is a proof by example of existence of the blueshifting effect, not a model of a real GRB!**



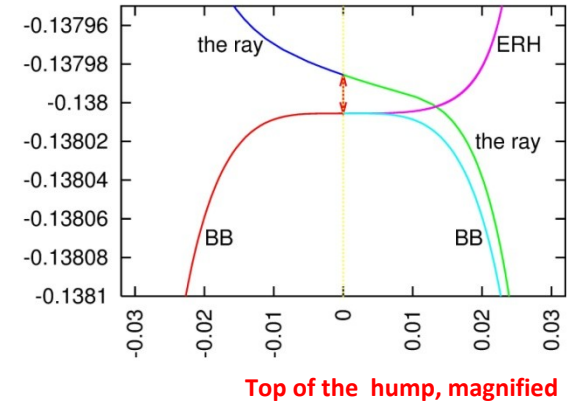
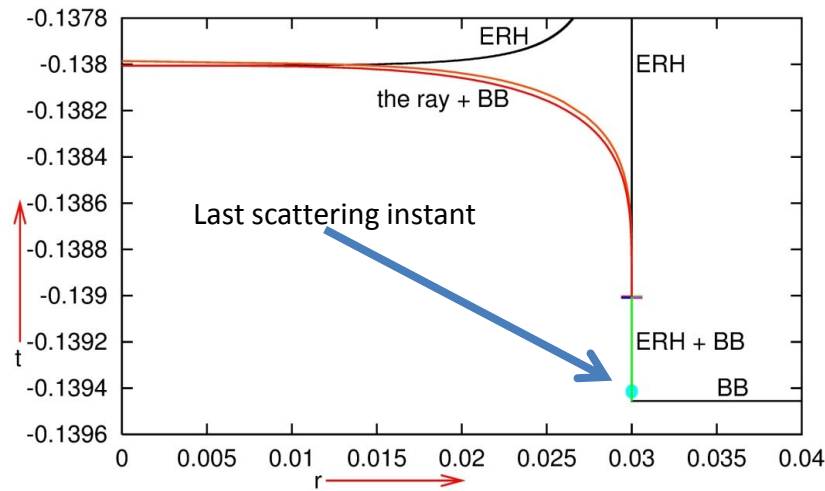
Here two humps are drawn in proportion to the age of the Universe

The lower hump (with ray 2) mimics a GRB source of the lowest observed energy.

Its height is  $8.9 \times 10^{-4} \times (\text{the } \Lambda\text{CDM age of the Universe}) \approx 1.23 \times 10^7 \text{ years}$ ,

it encompasses the mass  $\approx 3.1 \times 10^6$  masses of our Galaxy.

The other hump is 11.5 times higher and 2 times wider, and mimics a GRB source of the highest observed energy.



## The real profile of the hump, and the maximally blueshifted ray near the BB

Backward in time along the ray,  $z$  increases up to the first intersection with the ERH.

Further down,  $z$  decreases until the ray intersects the ERH again or until it hits the BB.

The hump parameters are chosen such that

$$2.5 \times 10^{-8} < 1 + z_{\text{observed now}} < 1.7 \times 10^{-5}$$

which moves the frequencies from the hydrogen emission range to the GRB range:

$$0.24 \times 10^{19} < \nu_{\text{GRB}} < 1.25 \times 10^{23} \text{ Hz.}$$



QSS models of this type reproduce [14,15]:

- (1) The observed frequency range of the GRBs ( $0.24 \times 10^{19} \text{Hz} \leq \nu \leq 1.25 \times 10^{23} \text{Hz}$ );
- (2) The duration of the GRBs (up to 30 hours, mostly  $\approx 2$  min) – see next page;
- (4) Collimation of GRBs into narrow jets;
- (5) The large distances to their sources ( $n \times 10^9$  ly);
- (6) The multitude of the GRBs (observed:  $\approx 1/\text{day}$ )  
by putting many BB humps into a Friedmann background.

At the current resolution of detectors ( $0.5^\circ$ ) 44,000 GRB sources would fill the whole sky.

In the currently best QSS model this number is  $11\,005 < N < 11\,014$ .

The remaining property:

- (3) The duration of afterglows (observed: up to  $n \times 100$  days, typically a few) is still to be dealt with,  
but the afterglows necessarily exist.

[14] A. Kasiński, Properties of blueshifted light rays in quasi-spherical Szekeres metrics. *Phys. Rev.* **D97**, 064047 (2018).

[15] A. Kasiński, Cosmological blueshifting may explain the gamma ray bursts. *Phys. Rev.* **D93**, 043525 (2016).

## 9. Explaining the brief durations of the gamma-flashes

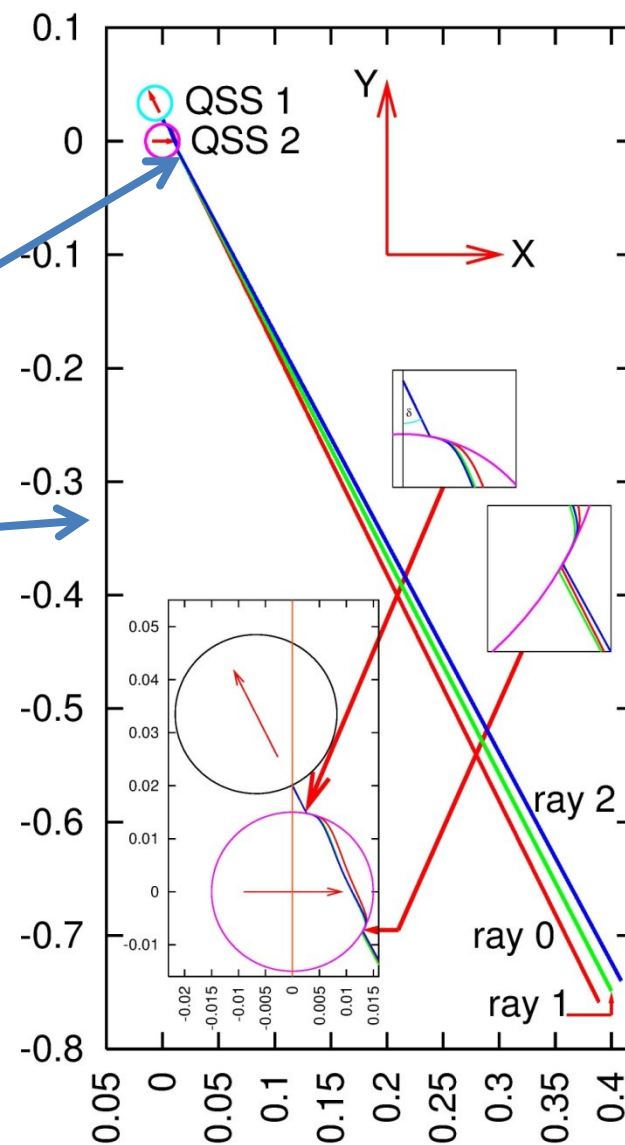
This is explained by means of the drift effect [16,17,18].

The maximally blueshifted ray emitted in QSS1 propagating over a second BB hump (QSS2) is *deflected*, and *the angle of deflection changes with time*.

→ *The ray will miss the observer after a while.*

In this configuration the current observer would not see any gamma ray from QSS1 10 minutes after the arrival of the first flash [19].

Instead, she would see UV rays (the afterglow!) from the same direction.



[16] A. Krasinski and K. Bolejko, Redshift propagation equations in the  $\beta' \neq 0$  Szekeres models. *Phys. Rev.* **D83**, 083503 (2011).

[17] M. Korzyński and J. Kopiński, Optical drift effects in general relativity. *J. Cosm. Astropart. Phys.* **03**, 012 (2018).

[18] C. Quercellini, L. Amendola, A. Balbi, P. Cabella, M. Quartin, Real-time cosmology. *Phys. Rep.* **521**, 95 -- 134 (2012).

[19] A. Krasinski, Short-lived flashes of gamma radiation in a quasi-spherical Szekeres metric. ArXiv 1803.10101, submitted for publication.

## 10. Expression of hope

Most astronomers treat inhomogeneous models as an enemy to kill.

Example [18]: Gaia or E-ELT could distinguish between FLRW and L-T  
``*possibly eliminating an exotic alternative explanation to dark energy*''.

(Is a lumpy mass distribution really exotic? This is all there is to L-T and Sz models. On the other hand, you cannot buy dark energy in a local shop. [As Jürgen Ehlers would probably say.])

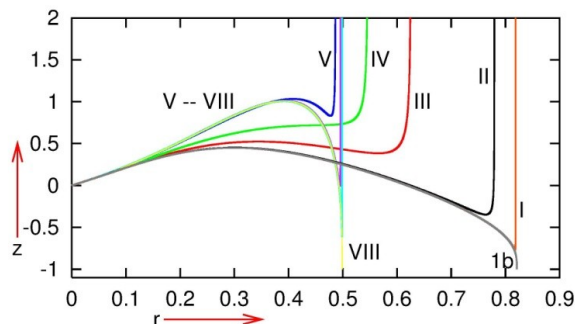
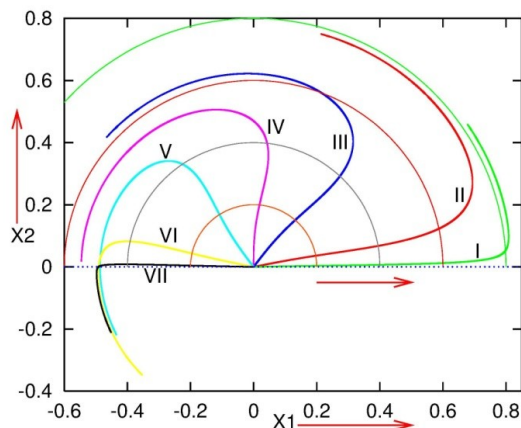
But L-T and Szekeres models imply interesting processes – and do it within the exact Einstein theory.

History of science teaches us that if a well-tested theory predicts a phenomenon, then the prediction has to be taken seriously, thoroughly investigated, then put to experimental tests.

I did my work with the hope that this will happen with the results reported here (but will I live long enough to see it?).

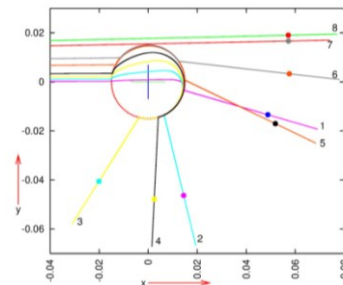
## 11. Appendix: Blueshifts in exemplary QSS models

In an *axially symmetric* QSS model, a *necessary condition* for infinite blueshift is that the ray is *axial* (intersects every space of constant  $t$  on the symmetry axis) [11].



Rays 1b and VIII are axial.

Rays overshooting the hump would be strongly deflected and would hit the BB in the Friedmann region with  $z_{\text{obs}} = \infty$ .



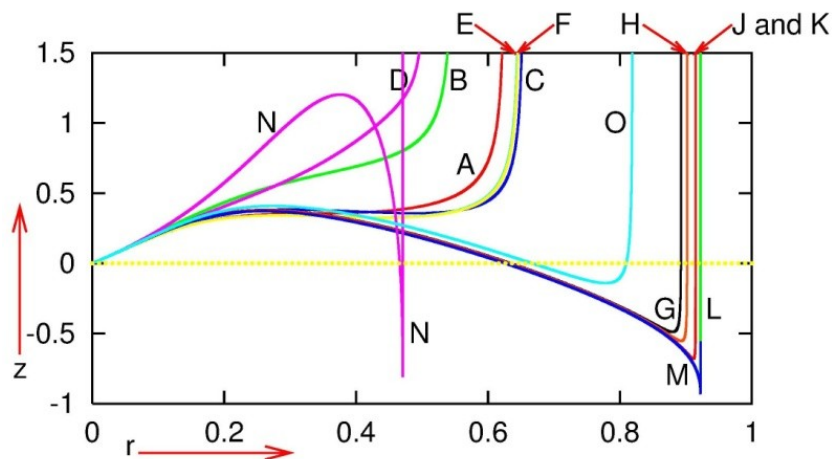
**Rays projected on a surface of constant  $t$  and  $\varphi$  and  $z$ -profiles along them**

$z_{\text{min}} \rightarrow -1$  when the ray approaches axial.

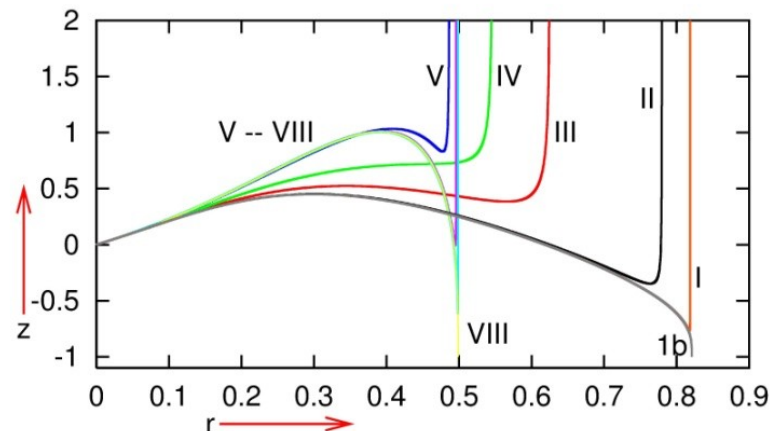
On rays 1b and VIII,  $1 + z_{\text{min}} < 10^{-5}$ .

Non-axial rays hit the BB hump tangentially to  $r = \text{constant}$  surfaces, with  $z_{\text{obs}} \rightarrow \infty$  (the same happens with nonradial rays in L-T).

In a fully nonsymmetric QSS model two opposite null directions exist along which the blueshift is near to -1 [11].



On approaching a preferred direction in a nonsymmetric QSS model the redshift profiles behave similarly



to the redshift profiles on rays approaching the axial direction in an axially symmetric QSS

But these directions *do not* coincide with the two principal null directions of the Weyl tensor, except in the axially symmetric case [11].

In the now-best Szekeres/Friedmann model [11], the angular radius of a GRB source is  $0.9681^\circ < \vartheta < 0.9783^\circ$ , depending on the direction of observation.

The current precision in determining the direction to an observed GRB source is a disk in the sky of radius  $\approx 0.5^\circ$ .

Thus, the whole sky could accommodate

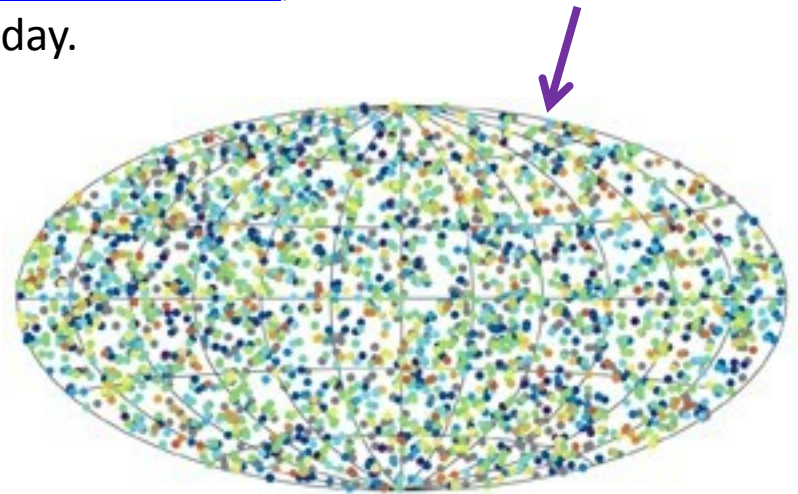
$$11\,005 < N < 11\,014$$

such objects.

The BATSE detector ([Burst And Transient Source Experiment](#)) detected 2704 GRBs between 1991 and 1999 [19] – this is nearly 1 per day.

So, during the 27 years from 1991 to now **8112** GRBs should have been discovered .

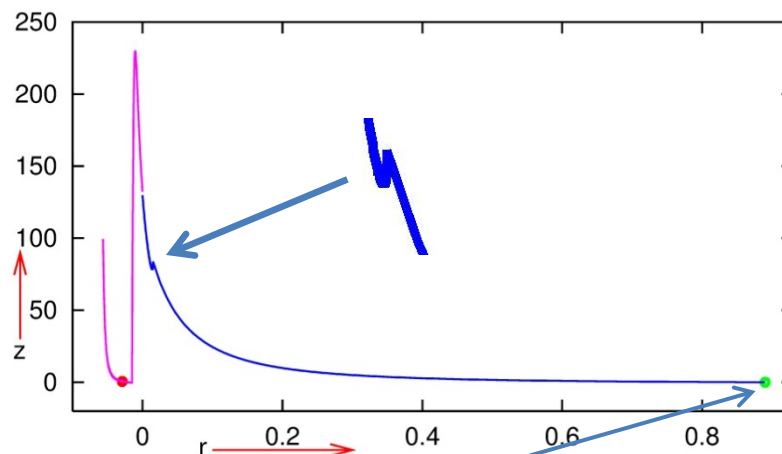
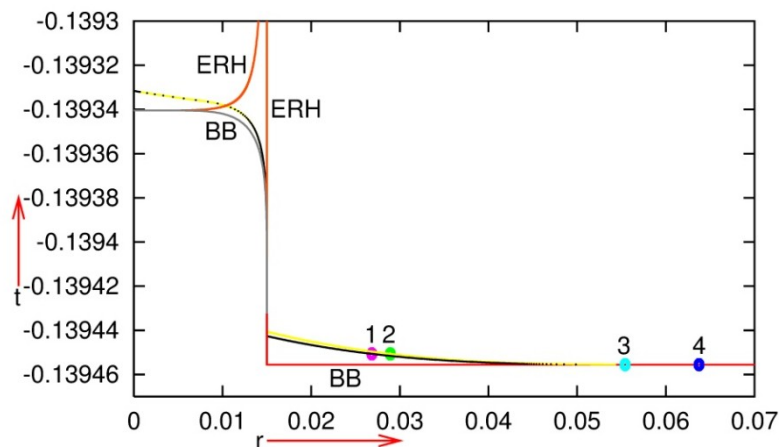
→ The **numbers** in the model and in the observations are not in contradiction.



[11] A. Kasiński, Properties of blueshifted light rays in quasi-spherical Szekeres metrics. *Phys. Rev.* **D97**, 064047 (2018).

[19] Gamma-Ray Bursts, [http://swift.sonoma.edu/about\\_swift/grbs.html](http://swift.sonoma.edu/about_swift/grbs.html)

When local blueshifts are present, *redshift fails* to be a distance indicator [16].



$z(r)$  seen by the observer at  $r \approx 0.9$

calculated along the **yellow ray**.

The redshift first increases toward the past, then decreases under the ERH.

At the **red dot** in the right graph  $z = 0.598$ .

The standard formula implies that source to lie  $5.9 \times 10^9$  years to the past [17,18].

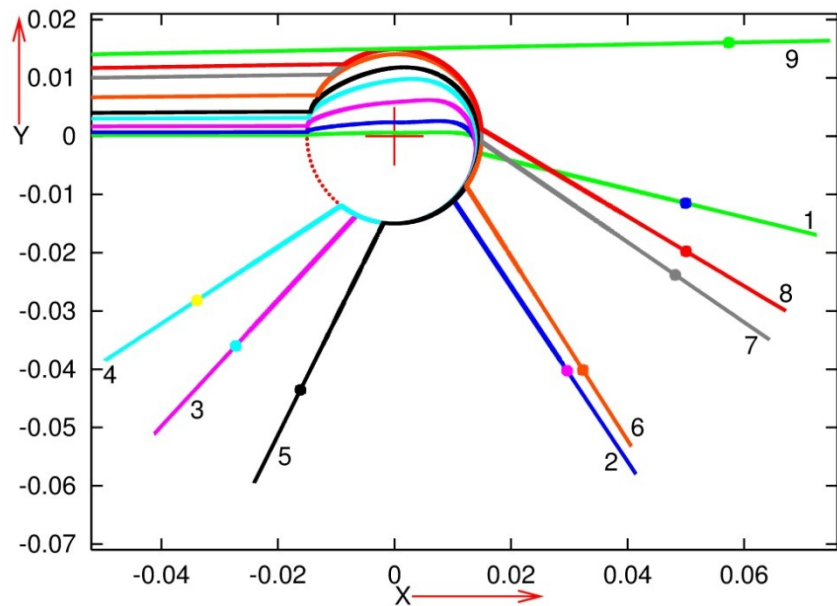
In this model, the source lies  $1.37 \times 10^{10}$  years to the past.

[16] A. Kasiński, Properties of blueshifted light rays in quasi-spherical Szekeres metrics. *Phys. Rev.* **D97**, 064047 (2018).

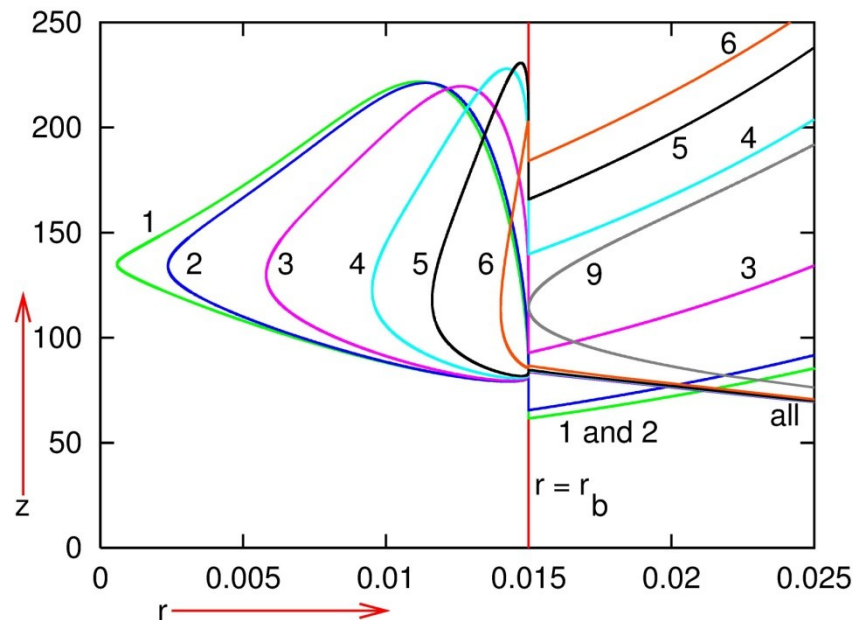
[17] E. L. Wright, A Cosmology Calculator for the World Wide Web. *Publ. Astr. Soc. Pac.* **118**, 1711 (2006).

[18] E. L. Wright, <http://www.astro.ucla.edu/~wright/ACC.html>

## Examples of non-monotonic redshift along non-axial rays:



Rays overshooting the BB hump of a QSS region  
The observer is at  $X \approx -0.9$ , far at left.



and  $z(r)$  profiles along them [16].  
The observer is at  $r \approx 0.9$ , far at right.